Soft Matter

View Online
Dynamic Article Links

Cite this: *Soft Matter*, 2011, **7**, 8657

www.rsc.org/softmatter

PAPER

Mechanics of reversible adhesion

Jian Wu,[a] Seok Kim,[b] Weiqiu Chen,[c] Andrew Carlson,[b] Keh-Chih Hwang,[a] Yonggang Huang*[d] and John A. Rogers*[be]

Received 17th May 2011, Accepted 5th July 2011
DOI: 10.1039/c1sm05915g

By pressure-controlled surface contact area, reversible adhesion can be achieved with strengths tunable by 3 orders of magnitude. This capability facilitates robust transfer printing of active materials and devices onto any surface for the development of stretchable and/or curvilinear electronics. The most important parameter in designing the surfaces of stamps for this process is the height of the microtips relief: tall microtips may fail to pick up electronics from their growth substrate, while short ones may fail to print electronics on the receiver substrate. Mechanics models are developed to determine the range of the microtip height for successful transfer printing. Analytical expressions for the minimum and maximum heights are obtained, which are very useful for stamp design.

1. Introduction

Geckos are masters at sticking and unsticking to surface of all kinds because their feet have fibrillar structures to adjust adhesion with a surface. This capability has motivated extensive research on biomimetic adhesion materials,[1–17] though fibrillar structures can be difficult to realize for synthetic materials. Aphids, on the other hand, use sagging and retraction of foot pads to enlarge or diminish contact area with a surface to modulate adhesion. This inspired Kim *et al.*[18] to achieve reversible adhesion by adjusting the surface contact area, and facilitated the use of the resulting concepts in transfer printing of silicon platelets onto nearly any type of surface. As illustrated in Fig. 1, a square polydimethylsiloxane (PDMS) stamp with pyramid-shaped microtips at each corner was fabricated to pick up silicon platelets from their growth substrate, and print (release) them onto a receiver substrate. The entire stamp (including microtips) collapsed onto a silicon platelet to reach a maximum contact area when the PDMS stamp was pressed firmly against the platelet. Rapid retraction of the PDMS stamp then lifted the platelet from its supporting substrate, after which the microtips gradually resumed their original shape due to the viscoelasticity of PDMS, leaving contact with the platelet only at the sharp tips of the pyramids, corresponding to very small contact areas. In this configuration, the platelet can then be easily transferred to a receiver surface, as demonstrated by transfer printing of silicon platelets and membranes onto rough or non-adhesive surfaces.[18]

The important parameters in stamp design for transfer printing (and reversible adhesion) are the microtip height h_{microtip}, width w_{microtip} and stamp width w_{stamp} (Fig. 1b). When firmly compressed, a stamp with tall microtips (*i.e.*, large h_{microtip}) experiences a large elastic restoring force, and may fail to pick up silicon platelets from their growth substrate. For short microtips (*i.e.*, small h_{microtip}), however, the elastic restoring force is too small to overcome the adhesion between the stamp and platelets such that the microtips do not resume their original shape, and the stamp may fail to print silicon platelets onto the receiver substrate.

This paper determines analytically the range of microtip height (and width) for successful transfer printing (and reversible adhesion). It begins with two-dimensional (2D) models for minimum and maximum heights of microtips in Sections 2 and 3, respectively, and identifies the underlying mechanism of deformation and establishes a scaling law for stamp design and fabrication. Section 4 gives the results for three-dimensional (3D) models, and compares with experiments.[18] Simple, analytical expressions for the minimum and maximum heights of microtips and the scaling laws are obtained analytically, which are very useful to stamp design, while Kim *et al.*[18] only obtained numerical results.

2. 2D model for minimum height h_{min} of microtips

At the minimum height h_{min}, the compressive preload is completely released such that h_{min} is governed by the adhesion energy between the stamp and platelet, and the strain energy

[a]*AML, Department of Engineering Mechanics, Tsinghua Universitry, Beijing 100084, China*
[b]*Department of Materials Science and Engineering, Beckman Institute, and Seitz Materials Research Laboratory, University of Illinois, Urbana, Illinois, 61801, USA. E-mail: jrogers@illinois.edu*
[c]*Soft Matter Research Center, Zhejiang University, Hangzhou 310027, China*
[d]*Department of Civil and Environmental Engineering and Department of Mechanical Engineering, Northwestern University, Evanston, Illinois 60208, USA. E-mail: y-huang@northwestern.edu*
[e]*Departments of Chemistry, Electrical and Computer Engineering, and Mechanical Science and Engineering, University of Illinois, Urbana, Illinois, 61801, USA*

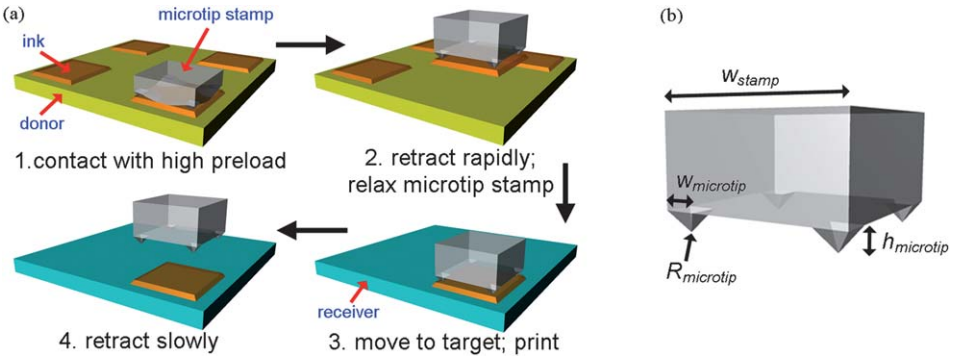

Fig. 1 (a) Implementation of elastomeric, microtip adhesive surface in a stamp for deterministic assembly by transfer printing. (b) Elastomeric, microtip adhesive surface consisting of four features of microtip relief on the surface of square post.

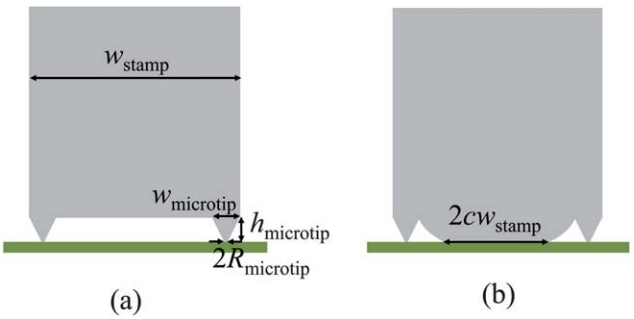

Fig. 2 A schematic diagram for the 2D model: (a) original stamp and (b) collapsed stamp.

$U_{collapse}$ due to stamp collapse onto the platelet. Fig. 2 shows the 2D model for h_{min}; the stamp has microtips on a flat post; the microtips have height $h_{microtip}$, width $w_{microtip}$, tip radius $R_{microtip}$, and spacing which equals the stamp width w_{stamp}. The post collapses onto the platelet over a length $2cw_{stamp}$ due to adhesion, where $2c$ represents the percentage of collapse on the stamp surface. The total potential energy is

$$U_{total} = U_{collapse} - 2cw_{stamp}\gamma, \tag{1}$$

where γ is the work of adhesion. Huang *et al.*[19] obtained the strain energy accounting for the large elastic mismatch between the PDMS stamp and silicon platelet, as

$$U_{collapse} = \frac{\overline{E}h_{microtip}^2}{2}\frac{K(2c)}{K\left(\sqrt{1-4c^2}\right)} \tag{2}$$

for a small tip radius $R_{microtip} \ll w_{stamp}$, where $\bar{E} = 4E/3$ is the plane-strain modulus of the stamp (and E is the Young's modulus), and K is the complete elliptic integral of first kind. The above equation is modified to account for the finite stamp width as (see Appendix for details)

$$U_{collapse} = \frac{1}{1.07\ln\left(\frac{w_{stamp}}{R_{microtip}}\right) - 1.90}\frac{\overline{E}h_{microtip}^2}{2}\frac{K(2c)}{K\left(\sqrt{1-4c^2}\right)}. \tag{3}$$

The percentage of collapse $2c$ is determined by minimizing the total potential energy $dU_{total}/dc = 0$, which gives

$$\frac{d}{dc}\left[\frac{K(2c)}{K\left(\sqrt{1-4c^2}\right)}\right] = \left[1.07\ln\left(\frac{w_{stamp}}{R_{microtip}}\right) - 1.90\right]\frac{4\gamma w_{stamp}}{\overline{E}h_{microtip}^2}; \tag{4}$$

therefore c depends on $R_{microtip}/w_{stamp}$ and the ratio of adhesion energy to strain energy due to collapse, $4\gamma w_{stamp}/\bar{E}h^2_{microtip}$. The total potential energy U_{total} in eqn (1) also depends on $R_{microtip}/w_{stamp}$ and $4\gamma w_{stamp}/\bar{E}h^2_{microtip}$.

The minimal height h_{min} of microtips is reached when U_{total} equals the energy without stamp collapse nor adhesion, and the latter is zero. For $h_{microtip} > h_{min}$, U_{total} is positive such that the stamp does not collapse onto the platelet upon complete release of the compressive preload. This gives the minimum height of microtips as

$$h_{min} \approx \sqrt{\left[1.52\ln\left(\frac{w_{stamp}}{R_{microtip}}\right) - 2.69\right]\frac{\gamma w_{stamp}}{\overline{E}}}. \tag{5}$$

It is linearly proportional to the square root of stamp width, adhesion energy, and reciprocal of stamp modulus, and also depends on the microtip radius.

3. 2D model for maximum height h_{max} of microtips

At the maximum height h_{max} the stamp may fail to pick up the platelet because the collapsed stamp starts to delaminate from the silicon platelet upon rapid retraction of the stamp, which is equivalent to a reversal of the (compressive) preload P/w_{stamp} (force per unit width in the 2D model). The gap between the stamp and platelet can be modeled as two cracks near free edges (Fig. 2b). The crack tip energy release rate, accounting for large elastic mismatch between the PDMS stamp and silicon platelet, is obtained analytically in the Appendix as

$$G = \frac{0.415}{1.07\ln\left(\frac{w_{stamp}}{w_{microtip}}\right) - 0.42}\frac{\overline{E}h'^2}{w_{stamp}}, \tag{6}$$

where h' is the reduced height of microtips due to the preload P. At the maximum height h_{max} of microtips the energy release rate reaches the work of adhesion γ such that the collapsed stamp delaminates from the platelet. This gives

$$h' = 1.55\sqrt{\left[1.07\ln\left(\frac{w_{\text{stamp}}}{w_{\text{microtip}}}\right) - 0.42\right]\frac{\gamma w_{\text{stamp}}}{\overline{E}}}. \quad (7)$$

In the following h' is related to the microtip height h_{microtip}, which, together with the above equation, then gives $h_{\max}$.

Once the post collapses onto the platelet, further increase in P reduces the crack tip energy release rate (or equivalently the stress intensity factor), but the post-platelet contact area does not change until the energy release rate reaches zero, after which the contact area increases with the preload, and crack length decreases, *i.e.* "zipping of the interface". Vanishing of the crack tip stress intensity factor gives (see Appendix for details)

$$\sqrt{1.07\ln\left(\frac{w_{\text{stamp}}}{w_{\text{microtip}}}\right) - 0.42}\,\frac{P}{\overline{E}w_{\text{stamp}}h_{\text{microtip}}}\sqrt{c_{\max}(1+2c_{\max})}(1-2c_{\max})K\left(\sqrt{1-4c_{\max}^2}\right)$$

$$-\int_0^1 \exp\left[\frac{-P}{2\overline{E}w_{\text{stamp}}}\,\frac{1+2c_{\max}-2\sqrt{c_{\max}(1+2c_{\max})}+\dfrac{\sqrt{c_{\max}(1+2c_{\max})}(1-2c_{\max})}{\sqrt{1.07\ln\left(\frac{w_{\text{stamp}}}{w_{\text{microtip}}}\right)-0.42}}K(2c_{\max})}{w_{\text{microtip}}x+2R_{\text{microtip}}(1-x)}\right]\mathrm{d}x = 0. \quad (12)$$

$$\frac{1}{\sqrt{1.07\ln\left(\frac{w_{\text{stamp}}}{w_{\text{microtip}}}\right)-0.42}}$$

$$\times\frac{\overline{E}h'}{2}\sqrt{\frac{\pi}{c_{\max}w_{\text{stamp}}(1-4c_{\max}^2)}}\,\frac{1}{K\left(\sqrt{1-4c_{\max}^2}\right)}$$

$$-\frac{P}{2}\sqrt{\frac{\pi(1-2c_{\max})}{w_{\text{stamp}}^3}} = 0, \quad (8)$$

where $2c_{\max}$ is the maximum percentage of collapse for the preload P; the first (positive) term on the left side of eqn (8) is the stress intensity factor due to post collapse of height h', and the second (negative) term results from the compressive preload.

Finite-deformation analysis of microtips gives h' in terms of the force F_{microtip} in each microtip by (see Appendix for details)

$$\frac{h'}{h_{\text{microtip}}} = \int_0^1 \exp\left\{\frac{F_{\text{microtip}}}{\overline{E}w_{\text{stamp}}\left[w_{\text{microtip}}x+2R_{\text{microtip}}(1-x)\right]}\right\}\mathrm{d}x. \quad (9)$$

Force equilibrium relates F_{microtip} to the preload P by

$$2F_{\text{microtip}} + F_{\text{post}} = -P \quad (10)$$

where F_{post} is the force on the collapsed post, and is obtained in the Appendix as

$$F_{\text{post}} = \frac{\overline{E}w_{\text{stamp}}h'}{1.07\ln\left(\frac{w_{\text{stamp}}}{w_{\text{microtip}}}\right)-0.42}\,\frac{K(2c_{\max})}{K\left(\sqrt{1-4c_{\max}^2}\right)} - 2P\left[\sqrt{c_{\max}(1+2c_{\max})}-c_{\max}\right]. \quad (11)$$

Elimination of h', F_{microtip} and F_{post} from eqn (8)–(11) gives

Eqn (7) holds for the maximum height $h_{\max}$ of microtips. Its substitution into eqn (8) gives the equation for $c_{\max}$

$$\sqrt{c_{\max}(1+2c_{\max})}(1-2c_{\max})\,K\left(\sqrt{1-4c_{\max}^2}\right) = 1.55\frac{\sqrt{\gamma\overline{E}w_{\text{stamp}}^3}}{P}. \quad (13)$$

Its substitution into eqn (12) gives analytically the maximum height $h_{\max}$ of microtips aswhere $c_{\max}$ is obtained numerically from eqn (13). The maximum height of microtips scales with the square root of stamp width, adhesion energy, and reciprocal of

$$h_{\max} = \frac{\sqrt{\left[2.57\ln\left(\frac{w_{\text{stamp}}}{w_{\text{microtip}}}\right)-1.01\right]\frac{\gamma w_{\text{stamp}}}{\overline{E}}}}{\displaystyle\int_0^1 \exp\left[\frac{-P}{2\overline{E}w_{\text{stamp}}}\,\frac{1+2c_{\max}-2\sqrt{c_{\max}(1+2c_{\max})}+\dfrac{\sqrt{c_{\max}(1+2c_{\max})}(1-2c_{\max})}{\sqrt{1.07\ln\left(\frac{w_{\text{stamp}}}{w_{\text{microtip}}}\right)-0.42}}K(2c_{\max})}{w_{\text{microtip}}x+2R_{\text{microtip}}(1-x)}\right]\mathrm{d}x}, \quad (14)$$

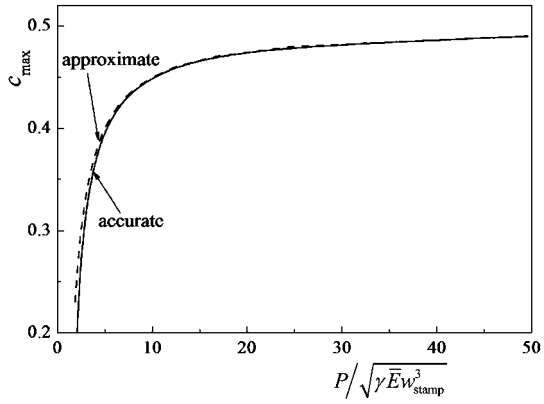

Fig. 3 c_{max} *versus* the normalized preload $P/\sqrt{\gamma \bar{E} w_{stamp}^3}$ for 2D accurate and approximate solutions, where $2c_{max}$ is the maximum percentage of collapse, P is the preload, γ is the work of adhesion of the PDMS/silicon interface, $\bar{E}$ is the plane-strain modulus of PDMS, and w_{stamp} is the stamp width.

stamp modulus, and also depends on the preload and microtip width and tip radius.

As shown in Fig. 3, eqn (13) has an excellent approximate solution obtained from the asymptotic analysis for $P \gg \sqrt{\gamma \bar{E} w_{stamp}^3}$,

$$1 - 2c_{max} = \frac{0.987\sqrt{\gamma \bar{E} w_{stamp}^3}}{P}. \quad (15)$$

Its substitution into eqn (14) then gives the analytical solution of the maximum height of microtips.

The analysis can be significantly simplified by approximating each microtip as a uniform column of equal height $h_{microtip}$ and volume. For sharp microtips $R_{microtip} \ll w_{microtip}$, these give the equivalent width of the column $w_{microtip}/2$. Finite-deformation analysis of the column gives

$$\frac{h'}{h_{microtip}} = \exp\left(\frac{2F_{microtip}}{\bar{E} w_{stamp}\, w_{microtip}}\right) \quad (16)$$

to replace eqn (9). The maximum height of microtips is then simplified to

$$h_{max} = \sqrt{\left[2.57 \ln\left(\frac{w_{stamp}}{w_{microtip}}\right) - 1.01\right]\frac{\gamma w_{stamp}}{\bar{E}}} \times \exp\left\{0.494\sqrt{\frac{\gamma w_{stamp}}{\bar{E} w_{microtip}^2}}\left[1 + \frac{2.08 + \ln\left(\frac{P}{\sqrt{\gamma \bar{E} w_{stamp}^3}}\right)}{\sqrt{1.07 \ln\left(\frac{w_{stamp}}{w_{microtip}}\right) - 0.42}}\right]\right\}, \quad (17)$$

where eqn (15) and the asymptotic expansion of the complete elliptic integral of first kind K for relatively large preload $P \gg \sqrt{\gamma \bar{E} w_{stamp}^3}$ have been used. As shown in Fig. 4 for the work of adhesion $\gamma = 0.155$ N m^{-1} of the PDMS/silicon

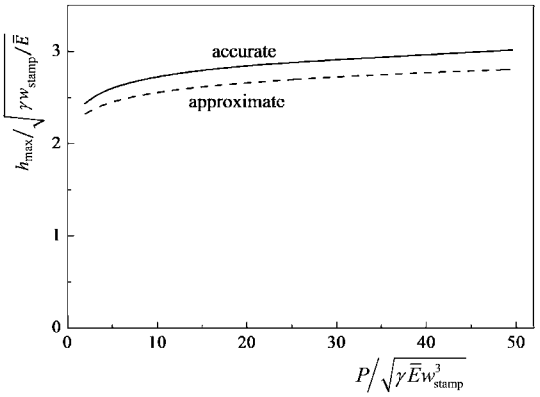

Fig. 4 The normalized maximum height of microtips $h_{max}/\sqrt{\gamma w_{stamp}/\bar{E}}$ *versus* the normalized preload $P/\sqrt{\gamma \bar{E} w_{stamp}^3}$ for 2D accurate and approximate solutions.

interface, plane-strain modulus $\bar{E} = 2.4$ MPa of PDMS, stamp width $w_{stamp} = 100$ μm and microtip width $w_{microtip} = 18$ μm, the analytical expression in eqn (17) is a very good approximation of the maximum height of microtips in eqn (14).

4. 3D models for minimum and maximum heights of microtips

Following the same approach as in Section 2 for 2D, Kim *et al.*[18] obtained the minimum height of microtips in 3D analysis, *i.e.*, one pyramid-shaped microtip at each corner of the square post. The minimum height of microtips was given by (see ESI of ref. 18)

$$h_{min} \approx \sqrt{\left[3.04 \ln\left(\frac{w_{stamp}}{R_{microtip}}\right) - 4.44\right]\frac{\gamma w_{stamp}}{\bar{E}}}. \quad (18)$$

Fig. 5 shows that the minimum height of microtips (normalized by $\sqrt{\gamma w_{stamp}/\bar{E}}$) decreases slowly as the normalized microtip radius $R_{microtip}/w_{stamp}$ increases. For the work of adhesion $\gamma = 0.155$ N m^{-1} of the PDMS/silicon interface, plane-strain modulus $\bar{E} = 2.4$ MPa of PDMS, stamp width $w_{stamp} = 100$ μm, and microtip radius $R_{microtip} = 750$ nm, eqn (18) gives the minimum height $h_{min} = 8.2$ μm. This agrees very well the experiments,[18]

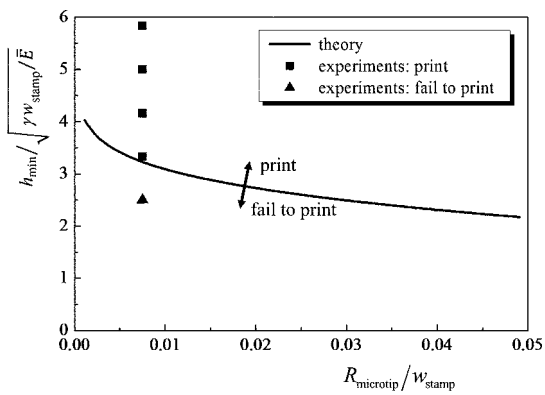

Fig. 5 The normalized minimum height of microtips $h_{min}/\sqrt{\gamma w_{stamp}/\bar{E}}$ *versus* the normalized microtip radius $R_{microtip}/w_{stamp}$ from 3D analysis.

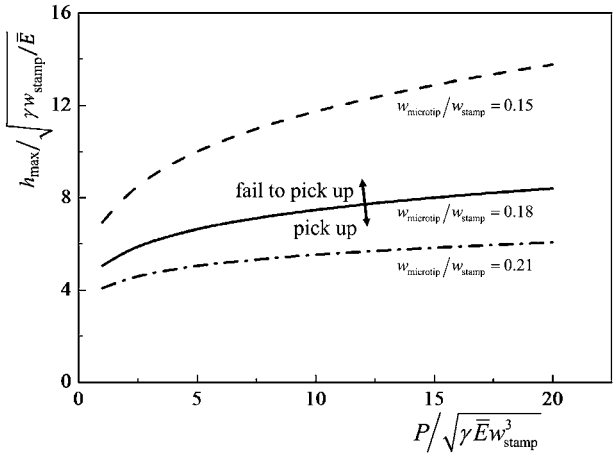

Fig. 6 The normalized maximum height of microtips $h_{max}/\sqrt{\gamma w_{stamp}/\bar{E}}$ *versus* the normalized preload $P/\sqrt{\gamma \bar{E} w_{stamp}^3}$ for several microtip-to-stamp width ratios from 3D analysis.

which successfully printed silicon platelets on the receiver substrate for the microtip height $h_{microtip} = 14.8$, 12.7, 10.6 and 8.5 μm, and failed to print for $h_{microtip} = 6.4$ μm.

Kim *et al.*[18] established the governing equations for the maximum height of microtips in 3D analysis (one pyramid-shaped microtip at each corner of the square post), but they only obtained numerical results. Following the same approach in Section 3 for 2D, we have obtained the analytical solution for the maximum height of microtips in 3D analysis as

$$h_{max} = \sqrt{\left[5.14 \ln\left(\frac{w_{stamp}}{w_{microtip}}\right) - 1.75\right]\frac{\gamma w_{stamp}}{\bar{E}}} \times \exp\left\{0.371\sqrt{\frac{\gamma}{\bar{E} w_{stamp}}}\left(\frac{w_{stamp}}{w_{microtip}}\right)^2\right\} \times \left[1 + \frac{2.08 + \ln\left(\frac{P}{\sqrt{\gamma \bar{E} w_{stamp}^3}}\right)}{\sqrt{2.14 \ln\left(\frac{w_{stamp}}{w_{microtip}}\right) - 0.73}}\right]\Bigg\}. \quad (19)$$

Fig. 6 shows that the normalized maximum height of microtips, $h_{max}/\sqrt{\gamma w_{stamp}/\bar{E}}$, increases slowly with the normalized preload $P/\sqrt{\gamma \bar{E} w_{stamp}^3}$. It also depends on the microtip-to-stamp width ratio $w_{microtip}/w_{stamp}$ and $\gamma/\bar{E} w_{stamp}$, the latter is 0.00065 in Fig. 6 (for $\gamma = 0.155$ N m^{-1}, $\bar{E} = 2.4$ MPa and $w_{stamp} = 100$ μm). As the microtip width decreases ($w_{microtip}/w_{stamp}$ decreasing from 0.21 to 0.15 in Fig. 6), the maximum height of microtips increases rapidly.

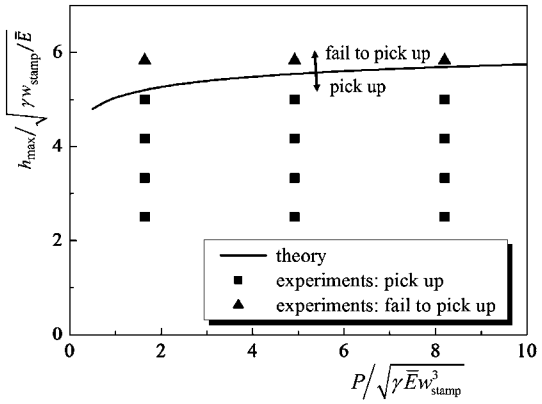

Fig. 7 The normalized maximum height of microtips with a fixed tip angle ($w_{microtip} = \sqrt{2} h_{microtip}$) *versus* the normalized preload $P/\sqrt{\gamma \bar{E} w_{stamp}^3}$ obtained from the analytical model and experiments.

The microtip width and height in experiments are related by $w_{microtip} = \sqrt{2}\, h_{microtip}$ since the microtip angle is fixed.[18] Eqn (19) then becomes

$$\frac{w_{stamp}}{h_{max}}\sqrt{\left[5.14 \ln\left(\frac{w_{stamp}}{h_{max}}\right) - 3.53\right]\frac{\gamma}{\bar{E} w_{stamp}}} \times \exp\left\{0.186\sqrt{\frac{\gamma}{\bar{E} w_{stamp}}}\left(\frac{w_{stamp}}{h_{max}}\right)^2\right\} \times \left[1 + \frac{2.08 + \ln\left(\frac{P}{\sqrt{\gamma \bar{E} w_{stamp}^3}}\right)}{\sqrt{2.14 \ln\left(\frac{w_{stamp}}{h_{max}}\right) - 1.47}}\right]\Bigg\} = 1, \quad (20)$$

which shows the normalized maximum height of microtips to depend only on $\gamma/\bar{E} w_{stamp}$ and the normalized preload $P/\sqrt{\gamma \bar{E} w_{stamp}^3}$. Fig. 7 compares the normalized maximum height of microtips in eqn (20) to the experimental data.[18] For $\gamma = 0.155$ N m^{-1}, $\bar{E} = 2.4$ MPa and $w_{stamp} = 100$ μm, the maximum height of microtip is 13.2, 14.1 and 14.4 μm for the preload $P = 0.001$, 0.003 and 0.005 N, respectively. This agrees very well the experiments,[18] which successfully picked up silicon platelets from the donor substrate for the microtip height $h_{microtip} = 6.4$, 8.5, 10.6 and 12.7 μm, and failed to pick for $h_{microtip} = 14.8$ μm for the same preloads $P = 0.001$, 0.003 and 0.005 N, as shown in Fig. 7.

5. Concluding remarks

Eqn (18) and (19) provide simple analytical expressions of the minimum and maximum heights of microtips. The minimum height, normalized by the work of adhesion for PDMS/silicon interface, plane-strain modulus of PDMS and stamp width *via* $\sqrt{\gamma w_{stamp}/\bar{E}}$, depends only on the ratio of microtip radius to stamp width. The maximum height shows a similar scaling law, and also depends on the preload and microtip width. These

analytical expressions agree very well with experiments,[18] and are useful to the stamp design for reversible adhesion.

Appendix

1. Stamp of finite width

The strain energy in eqn (2) for a stamp with infinite width equals to the work done by the stress traction over the collapsed post on the displacement (microtip height) h_{microtip}.[19] For a stamp with the finite width w_{stamp} but same microtip height h_{microtip}, the stress traction is reduced by a factor $1\Big/F\left(1-\frac{4R_{\text{microtip}}}{w_{\text{stamp}}}\right)$, where $4R_{\text{microtip}}$ is the total length of contact before collapse, and $F(x) = -0.071 - 0.535x + 0.169x^2 + 0.020x^3 - 1.071x^{-1}\ln(1-x)$ is obtained from the stress intensity handbook.[20] The strain energy for the stamp with finite width is reduced by the same factor. For small microtip radius $4R_{\text{microtip}} \ll w_{\text{stamp}}$, $F\left(1-\frac{4R_{\text{microtip}}}{w_{\text{stamp}}}\right) \approx 1.07\ln\left(\frac{w_{\text{stamp}}}{R_{\text{microtip}}}\right) - 1.90$, which leads to the strain energy in eqn (3).

2. Energy release rate during rapid retraction of the stamp

The crack propagates along the stamp/platelet interface during rapid retraction of the stamp, and the stress intensity factor is obtained analytically as[20]

$$\frac{1}{\sqrt{1.07\ln\left(\frac{w_{\text{stamp}}}{w_{\text{microtip}}}\right)-0.42}}\frac{\overline{E}h'}{2}\sqrt{\frac{\pi}{cw_{\text{stamp}}(1-4c^2)}}\frac{1}{K\left(\sqrt{1-4c^2}\right)} \tag{21}$$

where h' is the reduced height of microtips, $2c$ is the percentage of collapse, and the $\frac{1}{\sqrt{1.07\ln\left(\frac{w_{\text{stamp}}}{w_{\text{microtip}}}\right)-0.42}}$ is the factor for the finite width of the stamp. The crack tip energy release rate, accounting for large elastic mismatch between the PDMS stamp and silicon platelet, is

$$G = \frac{1}{1.07\ln\left(\frac{w_{\text{stamp}}}{w_{\text{microtip}}}\right)-0.42}\frac{\pi\overline{E}h'^2}{8w_{\text{stamp}}}\frac{1}{c(1-4c^2)K^2\left(\sqrt{1-4c^2}\right)}.$$

It reaches a minimum at $c = 0.169$, leading to the minimal energy release rate in eqn (6), which should be less than the work of adhesion γ to ensure successful pick up of the platelet.

3. Maximum percentage of collapse $2c_{\max}$

The first (positive) term in eqn (8) is the same as the stress intensity factor in eqn (21) except that c is replaced by $c_{\max}$. The second (negative) term in eqn (8) is the stress intensity factor $\sigma\sqrt{\pi a}$ for a crack of size $2a$ subjected to remote stress σ normal to the crack,[20] where $\sigma = -\frac{P}{w_{\text{stamp}}^2}$, and $2a = \left(\frac{1}{2}-c\right)w_{\text{stamp}} - \frac{1}{2}w_{\text{microtip}} \approx \left(\frac{1}{2}-c\right)w_{\text{stamp}}$ for small microtip width $w_{\text{microtip}} \ll w_{\text{stamp}}$.

The ratio of force F_{microtip} to cross-section area A in each microtip gives the stress, where A varies linearly from in the microtip. Since PDMS is (nearly) incompressible, the logarithmic strain in the microtip is then obtained. Its integration then gives the reduced height of microtips in eqn (9).

The force on the collapsed post F_{post} consists of three parts;

(i) post collapse with height h' gives $\overline{E}w_{\text{stamp}}h'\frac{K(2c_{\max})}{K\left(\sqrt{1-4c_{\max}^2}\right)}$,[20] and the factor $\frac{1}{1.07\ln\left(\frac{w_{\text{stamp}}}{w_{\text{microtip}}}\right)-0.42}$ accounts for the finite width of the stamp;

(ii) uniform remote field gives $-P2c_{max}$; and

(iii) uniform compression over the non-collapsed part of the post, $-2P\left[\sqrt{c_{\max}(1+2c_{\max})}-2c_{\max}\right]$.

The above three give the force in the post in eqn (11).

Acknowledgements

The work was supported by the NSF (OISE-1043143, ECCS-0824129), NSFC, NSSEFF and the DoE (DEF-G02-91ER45439). The printing and adhesion components used funding from a MURI program and the NSF (DMI-0328162).

References

1 E. Arzt, S. Gorb and R. Spolenak, *Proc. Natl. Acad. Sci. U. S. A.*, 2003, **100**, 10603–10606.
2 A. K. Geim, S. V. Dubonos, I. V. Grigorieva, K. S. Novoselov, A. A. Zhukov and S. Y. Shapoval, *Nat. Mater.*, 2003, **2**, 461–463.
3 M. Sitti and R. S. Fearing, *J. Adhes. Sci. Technol.*, 2003, **17**, 1055–1073.
4 H. Gao and H. Yao, *Proc. Natl. Acad. Sci. U. S. A.*, 2004, **101**, 7851–7856.
5 C. Majidi, R. E. Groff, K. Autumn, S. Baek, B. Bush, N. Gravish, R. Maboudian, Y. Maeno, B. Schubert, M. Wilkinson and R. S. Fearing, *Phys. Rev. Lett.*, 2006, **97**, 076103.
6 S. Kim and M. Sitti, *Appl. Phys. Lett.*, 2006, **89**, 261911.
7 S. Gorb, M. Varenberg, A. Peressadko and J. Tuma, *J. R. Soc. Interface*, 2007, **4**, 271–275.
8 S. Reddy, E. Arzt and A. del Campo, *Adv. Mater.*, 2007, **19**, 3833–3837.
9 D. Santos, M. Spenko, A. Parness, S. Kim and M. Cutkosky, *J. Adhes. Sci. Technol.*, 2007, **21**, 1317–1341.
10 J. Lee and R. S. Fearing, *Langmuir*, 2008, **24**, 10587–10591.
11 M. T. Northen, C. Greiner, E. Arzt and K. L. Turner, *Adv. Mater.*, 2008, **20**, 3905–3909.
12 L. Qu, L. Dai, M. Stone, Z. Xia and Z. L. Wang, *Science*, 2008, **322**, 238–242.
13 M. P. Murphy, B. Aksak and M. Sitti, *Small*, 2009, **5**, 170–175.
14 S. Kim, M. Sitti, T. Xie and X. Xiao, *Soft Matter*, 2009, **5**, 3689–3693.
15 H. E. Jeong, J.-K. Lee, H. N. Kim, S. H. Moon and K. Y. Suh, *Proc. Natl. Acad. Sci. U. S. A.*, 2009, **106**, 5639–5644.
16 H. Ko, J. Lee, B. E. Schubert, Y.-L. Chueh, P. W. Leu, R. S. Fearing and A. Javey, *Nano Lett.*, 2009, **9**, 2054–2058.
17 J. Lee, B. Bush, R. Maboudian and R. S. Fearing, *Langmuir*, 2009, **25**, 12449–12453.
18 S. Kim, J. Wu, A. Carlson, S. H. Jin, A. Kovalsky, P. Glass, Z. Liu, N. Ahmed, S. L. Elgan, W. Chen, P. M. Ferreira, M. Sitti, Y. Huang and J. A. Rogers, *Proc. Natl. Acad. Sci. U. S. A.*, 2010, **107**, 17095–17100.
19 Y. Huang, W. Zhou, K. J. Hsia, E. Menard, J.-U. Park, J. A. Rogers and A. G. Alleyne, *Langmuir*, 2005, **21**, 8058–8068.
20 *The Stress Analysis of Cracks Handbook*, ed. H. Tada, P. C. Paris and G. R. Irwin, Professional Engineering Publishing, 2000.